Nonlinear Reflection of Grazing Acoustical Shock Waves: Unsteady Transition from von Neumann to Mach to Snell-Descartes Reflections

By
BASKAR SAMBANDAM[1], FRANÇOIS COULOUVRAT[1]†, AND RÉGIS MARCHIANO[1]

[1] Laboratoire de Modélisation en Mécanique, Université Pierre et Marie Curie & CNRS (UMR 7607), 4 place Jussieu, 75252 Paris cedex 05, France.

(Received ?? and in revised form ??)

We study the reflection of acoustical shock waves grazing with a small angle over a rigid surface. Depending on the incidence angle and the Mach number, the reflection patterns are mainly categorized into two types, namely the regular reflection and the irregular reflection. In the present work, using the nonlinear KZ-equation, this reflection problem is investigated for extremely weak shocks as encountered in acoustics. A critical parameter, defined as the ratio of the sinus of the incidence angle to the square root of the acoustical Mach number, is naturally introduced. For step shocks, we recover the self-similar (pseudo-steady) nature of the reflection, which is well-know right from von Neumann's study. Four types of reflection as a function of the critical parameter can be categorized. Thus, we describe the continuous but nonlinear and non-monotonic transition from linear reflection (Snell-Descartes laws) to the weak von Neumann type reflection observed for almost perfectly grazing incidence. This last one is a new, one-shock regime, contrarily

† Email address: coulouvr@ccr.jussieu.fr

to the other already known two- (regular reflection) or three-shocks (reflection of von Neumann type) regimes. Hence, the transition yet resolves another paradox on acoustical shock waves also addressed by von Neumann in his classical paper. However, step shocks are quite unrealistic in acoustics. Therefore, we investigate the generalization of this transition for N-waves or periodic saw-tooth waves, which are more appropriate for acoustics. Our results show an unsteady reflection effect necessarily associated to the energy decay of the incident wave. This effect is the counterpart of step shock propagation over a concave surface. For a given value of the critical parameter, all the patterns categorized for the step shock may successively appear when propagating along the surface, starting from weak von Neumann type reflection, then gradually turning out to von Neumann reflection and finally evolving into nonlinear regular reflection. This last one will asymptotically results into linear regular reflection (Snell-Descartes). The transition back to regular reflection may be of two types, depending on whether a secondary reflected shock is observed or not. This last case, described here for the first time, appears to be related to the non-constant state behind the incident shock, which prevents secondary reflection.

---

1. Introduction

As soon as a plane shock wave of acoustical Mach number M_a impinges over a rigid inclined surface with a grazing angle θ ($0 < \theta < \pi/2$), it gives rise to a reflected shock. The incident and reflected shocks, as they propagate (for instance, from left to right as shown in figure 1) along the rigid surface, result in a reflection pattern which can be basically of two types, namely the regular and the irregular reflections (see Ben-Dor 1992). The type of reflection depends on the grazing angle and the strength of the incident

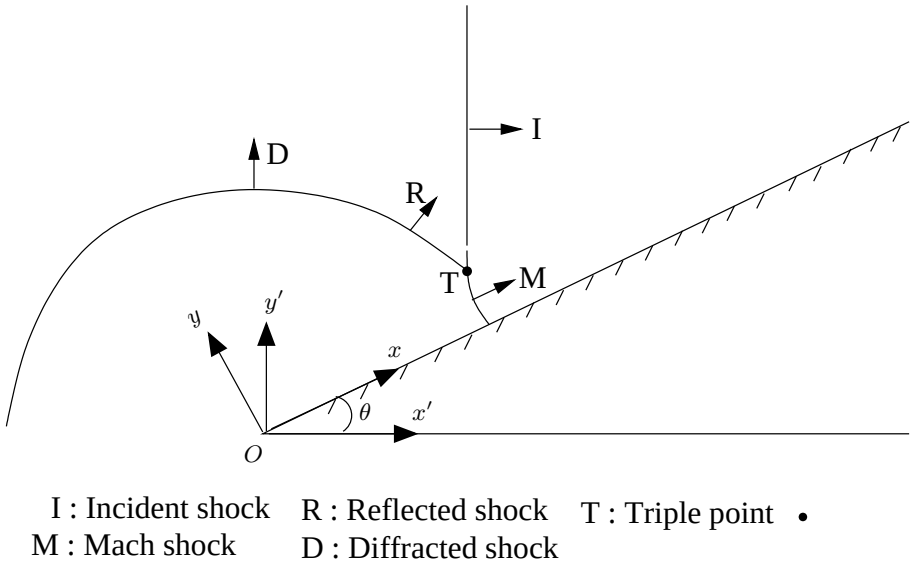

FIGURE 1. Reflection of a grazing wave: geometry of the physical problem.

shock. For a sufficiently large angle, or a sufficiently weak shock, the incident and the reflected shocks intersect right on the rigid surface. This type of reflection is called the *regular reflection*. As the angle decreases, or the shock amplitude increases, the point of intersection T of the incident and reflected shocks detaches from the surface. Due to the nonlinear interaction of these two shocks at T, a new shock emerges to ensure the contact with the surface. This emerging shock is called a *Mach shock* or *Mach stem*, and the point T of intersection of these three shocks is called the *Triple point*. This type of reflection is known as *irregular reflection*. For a strong incident shock, in addition to these three shocks at T, there exists also a contact discontinuity (slipstream). It divides the flow behind the reflected and the Mach shock into two states across which the normal velocity component and the pressure are continuous, whereas other quantities (tangential velocity, density, temperature, entropy) undergo a jump discontinuity. This is known as *Mach reflection* and is named after its first experimental observation by Mach (1878). This famous work of Mach has given birth to a new field of research commonly known as *shock wave reflection phenomena* (see Ben-Dor & Takayama 1992).

Theoretical investigation of the shock wave reflection was first carried out by von Neumann (1943) for inviscid perfect gases. His theory on irregular reflection is called *three-shock theory*, while the *two-shock theory* refers to regular reflection. The transition criteria between the two types of reflection are derived from these theories (see Henderson 1987). A basic assumption made in the derivation of these theories is the pseudo-steady (or self-similar) nature of the flow. These theories also assume all the waves in the flow are either shocks with negligible curvature separating constant states, or contact discontinuities with negligible thickness (slipstream).

The three-shock theory has a good agreement with experiments near the transition criteria when the incident shock Mach number is greater than 1.47, which is considered as a strong shock (see Colella & Henderson 1990). For weak shocks (incident shock Mach number less than 1.035), the three-shock theory leads to the conclusion that the Mach reflection is physically unrealistic while experimental evidence supported by numerical simulations (from inviscid Euler equations), shows that Mach reflection still remains possible for such weak shocks (see Colella & Henderson 1990). The discrepancy between the three-shock theory and the experimental studies has been referred as *von Neumann paradox*. The von Neumann paradox was first stated by Birkhoff (1950) and later more precisely by Colella & Henderson (1990). Several attempts have been made to resolve this paradox either experimentally or theoretically, with different proposed explanations. This nevertheless remains a challenging open problem.

For the case when the three-shock theory gives unrealistic results, Colella & Henderson (1990) observed numerically and experimentally a continuous slope of the shock front along the incident and the Mach shock. Their numerical results show that this continuous slope is because the reflected shock breaks down to a band of compressive waves as it approaches the incident shock and so that there is no triple point. They named this new

type of reflection the *von Neumann reflection*, which they introduced as a different regime from Mach reflection (where the slope has a discontinuity at the triple point as described by three-shock theory). Henderson, Crutchfield & Virgona (1997) provided computational and experimental evidence of the importance of viscosity and heat conductivity in the flow to solve the paradox. The boundary condition on the slipstream separating the two constant states behind the triple point has been questioned by Skews (1972) (also see Ben-Dor 1987; Kobayashi *et al.* 1995), and recently Kobayashi, Adachi & Suzuki (2004) gave experimental evidence for the non-self-similar nature of the weak Mach reflection. A singularity in the reflected shock curvature at the triple point shown by Sternberg (1959), or a singularity in the solution behind the triple point shown by Tabak & Rosales (1994) are other proposed explanations for the paradox. For more details on the literature of the paradox and also a detailed discussion of all possible types of reflection with their transition criteria, we refer to the recent review article by Ben-Dor & Takayama (1992). Hunter & Brio (2000) studied the weak shock reflection in the case of step shocks using the 2-dimensional Burgers' equation. This enabled them to capture a very tiny supersonic patch behind the triple point which was initially hypothesized by Guderley (1962). They also proved theoretically the existence of an expansion fan at the triple point in addition to the three shocks, which is yet another explanation for the paradox. Such a reflection pattern was first proposed by Guderley (1962) and is commonly known as *Guderley reflection*. From different numerical solvers of the Euler equations, Vasil'ev & Kraiko (1999) and Zakharian, Brio, Hunter & Webb (2000), respectively, captured the expansion fan and the supersonic patch. Tesdall & Hunter (2002) further investigated the problem and found (through a new numerical scheme developed by them) a more complex structure of the reflection pattern with a sequence of triple points along the Mach shock, each one associated to an additional expansion fan. This whole complex structure takes

place very locally in a tiny domain behind the leading triple point. Recently, Skews & Ashworth (2005) performed a very high-resolution experiment, which gives an evidence for the presence of a multi-reflection structure behind the three-shock reflection.

Extremely weak shock waves do exist in the acoustical regime corresponding to Mach numbers not much larger than 1.001 (while for instance experiments of Colella & Henderson (1990) do not go below Mach 1.035 and those of Skews & Ashworth (2005) below Mach 1.04). Examples of such shock waves are sonic boom in the atmosphere at the ground level, or ultrasonic shock waves produced by piezoelectric arrays in water for high frequency ultrasound therapy (such as lithotripsy). The objective of the present study is to investigate the nonlinear reflection of acoustical shock waves and to determine whether the reflection of extremely weak acoustical shock waves is specific or not. With this view point several unanswered questions arise. The first one is to investigate the different regimes of reflection of acoustical weak shock waves depending on the shock amplitude and the incidence angle. Though acoustical shock waves are extremely weak, they are nonetheless intrinsically nonlinear. However it remains uncertain whether nonlinear effects play a role at some stage during the reflection or, on the contrary, if acoustical shock waves still satisfy the linear Snell-Descartes laws of reflection. Indeed, von Neumann (1943) hypothesized acoustical shock waves behave differently from stronger shocks. The question is therefore to match the linear Snell-Descartes laws with weak shock theory. Another open question has also been pointed out by von Neumann (1943), who remarked that the linear Snell-Descartes laws themselves are singular. Indeed, they predict the well-known pressure doubling at the reflector surface, which is valid (in the linear theory) for any grazing angle except the perfectly grazing angle. For the perfectly grazing case, the incident shock wave propagates exactly parallel to the surface, there is no reflection at all and no pressure doubling. Therefore, even in the linear regime,

Snell-Descartes laws are singular, another paradox we suggest to call the *acoustical von Neumann paradox*. In his original paper, von Neumann conjectures for acoustical waves a smooth and monotonic transition between Snell-Descartes laws and perfectly grazing incidence, contrarily to the strong shock case. The first main objective of the present study is therefore to investigate this transition systematically.

Another key feature of acoustical shock waves is that they are never the perfect step shock between constant states that has been solely examined in the above cited studies. Indeed, acoustical shock waves are always preceded or followed by nonconstant flows which will modify the reflection structure. Also, acoustical shock waves are frequently not unique but appear as a sequence of two or more shocks. For instance, the sonic boom has typically the shape of an N-wave (two shocks) while long trains of ultrasound have the shape of a periodic saw-tooth wave. In all these cases, we expect the multiple incident and reflected shock waves to interact with one another. Our second main objective here is therefore to examine whether the categorization of the shock reflection regimes that is observed for the step shock, remains valid or not for other kind of acoustical shock waves.

In the case of a weak shock incident on the reflector with a small grazing angle, the wave propagation (whose direction is given by the normal to the wavefront as sketched on figure 1) is mostly oriented parallel to the reflecting surface. As the direction of propagation of the reflected wave will also deviate only slightly from the tangent to the reflector, this suggests that instead of the 2-dimensional Euler equations, the KZ-equation (see Zabolotskaya & Khokhlov 1969) may be used efficiently (section 2). Indeed, the KZ-equation is derived under two main assumptions: weak shocks and propagation in a preferred direction. Both of them are obviously well satisfied here, which makes the use of this equation especially well suited to the present case. Note this equation

is equivalent to the 2-dimensional Burgers' equation used by Hunter & Brio (2000). In the derivation of the boundary conditions for the KZ-equation, a critical parameter a is introduced naturally (section 3), which shows that the acoustical shock strength has to be of the order of the square of the grazing angle θ for full coupling between nonlinear and diffraction effects near the surface. A similar kind of parameter was also introduced by Hunter & Brio (2000). Then a self-similar rule is obtained for the step shock in the acoustical regime. The self-similar rule is also verified numerically in section 4. We also show that, unlike the nonlinear Fresnel diffraction (see Coulouvrat & Marchiano 2003), the flow for the N-wave or the periodic saw-tooth wave does not follow any self-similar law.

We then derive in section 5, a transition condition from regular to irregular reflection for the step shock, which is a general form of the detachment condition derived by Hunter (1991). By varying the critical parameter a, we study the different types of reflection starting from the linear regular reflection for a very large value of a (*Snell-Descartes reflection*) to the so-called *weak von Neumann reflection* for a small value of a, in which we observe a smooth reflected wave instead of a reflected shock. For intermediate values we recover the other regimes of reflection already found in the literature as described above. Such a complete "panorama" of the step shock reflection is the first main original result of this study and will enable us to solve the acoustical von Neumann paradox. The second one is given by the numerical study of the unsteady reflection phenomena in the case of N-waves and saw-tooth waves (section 6). In both cases, we obtain new results, which are not possible for step shocks grazing over a plane rigid surface, because the step shock reflection is self-similar. In particular, we observe non-monotonic trajectory of the triple-point. This leads to intricate reflection patterns such as inverse Mach reflection and transitioned regular reflection of two types, one of them being described here for

the first time. This type-two reflection has a behaviour similar to the unsteady reflection as discussed in Chapter 4 of Ben-Dor (1992) for step shocks grazing over a concave double wedge, but to our knowledge this is newly observed for the reflection of complex shock waveforms over a perfectly plane surface. Finally, we discuss the unsteady effects related to the decrease of energy of the incident shock wave along the reflecting plate. This unsteadiness will be shown to imply continuous transition from the initial nonlinear shock reflection regime at the tip of the plate, up to the final linear Snell-Descartes reflection.

2. Shock wave reflection and the KZ-equation

We consider a two-dimensional plane shock wave grazing over a plane rigid surface with acoustical Mach number M_a (defined as the ratio between the maximum amplitude of acoustical velocity V_0, which is the excess of the wave velocity on the constant sound velocity c_0 in the undisturbed medium, to the ambient sound speed). Typical values of this Mach number are about 10^{-3} for observed sonic booms (of Concorde) or ultrasonic shock waves. Note this corresponds in the usual definition of the Mach number to values smaller than 1.001, so much closer to 1 than the cases investigated previously in the literature (as mentioned in the introduction). The shock encounters a wedge of angle θ at point O as shown in figure 1. We assume a homogeneous and inviscid fluid of ambient density ρ_0. Let us take the longitudinal (normal to the incident wavefront) and the transverse (parallel to the incident wavefront) coordinates as x' and y' respectively. We denote the physical time by t and the oblique coordinates by (x, y) (respectively parallel and perpendicular to the reflecting surface) and fix the origin O at the tip of the wedge.

We define the dimensionless retarded time as $\tau' = \omega\,(t - x'/c_0)$, where ω is a reference angular frequency characteristic for the incident signal duration of periodicity. We make

the transverse and the longitudinal variables dimensionless by $Y' = y'/L$, $X' = x'/D$, where $L = 1/(k\sqrt{2\beta M_a})$ is the transverse length scale and $D = 1/(\beta k M_a)$ is the shock formation distance with $k = \omega/c_0$ the wave number and $\beta = 1 + B/2A$, B/A being the nonlinearity parameter (see Hamilton & Blackstock 1998). The dimensionless oblique coordinates and retarded time are defined similarly as $(X = x/D, Y = y/L)$ and $\tau = \omega\,(t - x/c_0)$.

We assume that (i) the grazing angle is small $\theta \ll 1$ (grazing wave assumption) and (ii) the shock wave is weak $M_a \ll 1$, which is appropriate for the acoustic case. These two assumptions justify the use of the paraxial approximation of the nonlinear wave equation, which is the well-known KZ-equation (see Zabolotskaya & Khokhlov 1969)

$$\frac{\partial^2 P}{\partial X \partial \tau} - \frac{\partial^2 P}{\partial Y^2} = \frac{\partial^2}{\partial \tau^2}\left(\frac{P^2}{2}\right), \tag{2.1}$$

where $P = p_a/(\rho_0 c_0 V_0)$ is the dimensionless acoustical pressure with p_a the acoustic pressure. We recall the KZ-equation is an approximation of the Euler equations valid for finite amplitude sound waves provided two main assumptions are satisfied. The first one requires waves of small amplitude; it is perfectly satisfied here for acoustical shocks according to the small values of the acoustical Mach number. The second one is the paraxial approximation, which assumes waves propagate mainly into a preferred direction, here the direction tangent to the reflector surface. In its linearized form, the dispersion relation of the KZ equation replaces the exact dispersion relation of the wave equation, which is a circle, by the parabola tangent to this circle at the main direction of propagation. This justifies the name of "parabolic approximation" which is frequently used instead of the "paraxial approximation". That approximation is estimated to be valid for directions of wave propagation that deviate from less than $\pm 30^o$, for which case the error in the dispersion equation is less than 1%. Here, we will study grazing angles for which the critical parameter introduced in the next section is typically less than 3, which

corresponds to angles less than 8.5^o in air and 14.5^o in water, so well within the range of validity of the paraxial approximation.

The KZ-equation can be expressed in the form of two conservation equations of the form

$$\frac{\partial P}{\partial X} = \frac{\partial U}{\partial Y} + \frac{\partial}{\partial \tau}\left(\frac{P^2}{2}\right), \tag{2.2}$$

$$0 = \frac{\partial P}{\partial Y} - \frac{\partial U}{\partial \tau}, \tag{2.3}$$

which can also be viewed as the weak disturbance asymptotic limit of the unsteady transonic problem (see Hunter 1991). Equation (2.2) is the well known 2-dimensional Burgers' equation, which takes care of the nonlinear effect, with equation (2.3) including the diffraction effect. Note however that when compared to the 2-dimensional Burgers' equation, the role of time and space have been interchanged in the KZ-equation, which takes the form of an evolution equation in space rather than in time. This interchange is allowed by the equivalence between time and space through the introduction of the retarded time as the "fast" variable in the multiple scales asymptotic process sustaining the derivation of the KZ-equation. An equivalent form but with evolution in time is known as the NPE-equation (see McDonald & Kuperman 1987)), which is strictly equivalent to the 2-dimensional Burgers' equation discussed by Hunter (1991). Note also that, because of this interchange between time and space, the computed solutions appear as a succession of views in the plane τ, Y with increasing X distances, instead of the more usual views in the plane X, Y with increasing times. Visually, on figures 3, 6 to 8, 11, 12, 14 and 16, this makes the incident field inclined towards the left, as it arrives earlier at positions more distant from the reflector surface. Similarly, the reflected field is inclined towards the right. To recover the usual viewpoint as sketched on figure 1, a horizontal symmetry of the above listed figures is simply to be performed.

The Rankine-Hugoniot condition for the system (2.2)-(2.3) is given by (see Coulouvrat & Marchiano 2003)

$$-W[P] = [U]N_Y + [P^2/2]N_\tau, \tag{2.4}$$

$$0 = [P]N_Y - [U]N_\tau, \tag{2.5}$$

where $[f] = f_2 - f_1$ is the notation for the jump of any quantity f across the shock, W is the shock normal speed and $\boldsymbol{N} = (N_\tau, N_Y)$ is the normal vector to the shock wave $\tau_s = \tau_s(X, Y)$, which is a curve in the (τ, Y) space evolving with the propagation variable X. Eliminating U from the above two jump relations, we get the shock condition as

$$-WN_\tau = N_Y^2 + \langle P \rangle N_\tau^2, \tag{2.6}$$

where $\langle P \rangle = (P_1 + P_2)/2$ is the mean value of P. The shock jump relations (2.4)-(2.5) and their alternate form (2.6) are used in finding the transition condition from regular to irregular reflection derived in section 5.1. We use the KZ-equation (2.1) to obtain the numerical results for the shock reflection problem in the (τ, Y) plane for a given X. This numerical problem needs the appropriate initial and boundary conditions, which will be examined in the next section.

3. The critical parameter and the boundary conditions

For computational purpose, it is convenient to work in the oblique coordinate system (x, y) in which x and y are parallel and perpendicular to the wedge surface respectively, as shown in figure 1. We denote the corresponding non-dimensional variables as (X, Y), and the corresponding retarded time as τ, as already defined in section 2.

The relation between the coordinates (X, Y) and (X', Y') is given by

$$X' = X\cos\theta - \frac{L}{D}Y\sin\theta = X + O(\sin^2\theta), \tag{3.1}$$

where L and D are defined in section 2. Here we make the fundamental assumption that

$\theta = O(\sqrt{M_a})$. For typical acoustical Mach numbers of order 10^{-3}, this corresponds to grazing angles of the order of a few degrees. The transformation $Y' \to Y$ can be defined similarly, but it is not used anywhere in our problem. The relation between the retarded times τ' and τ is given by

$$\tau' = \tau + aY + a^2 X + O(\sin^2\theta), \tag{3.2}$$

where the *critical parameter* a is naturally introduced as

$$a = \frac{\sin\theta}{\sqrt{2\beta M_a}} = O(1). \tag{3.3}$$

For numerical simulation, we have to prescribe the incoming wave at $X = 0$, from which we get the initial pressure field in the (τ, Y)-plane for the computation. This incoming field is the solution of the one dimensional Burgers' equation

$$\frac{\partial P}{\partial X'} - P\frac{\partial P}{\partial \tau'} = 0 \tag{3.4}$$

describing the propagation of a nonlinear plane wave in the X' direction.

In our problem, we study three types of waves, namely the step shock, the N-wave and the saw-tooth wave. We give the solution of the Burgers' equation in the (X', τ', Y')-variables for these three cases, and then transfer the solution to the (X, τ, Y)-variables using the transformations (3.1)-(3.3).

(i) Step Shock: The solution of the incoming field in the (X', τ', Y')-variables is given by

$$P(X', \tau', Y') = \begin{cases} 0, & \text{if } \tau' \leqslant -X'/2 \\ 1, & \text{if } \tau' > -X'/2 \end{cases} \tag{3.5}$$

and the solution of the incoming field in the (X, τ, Y)-variables is given by

$$P(X, \tau, Y) = \begin{cases} 0, & \text{if } \tau + aY + a^2 X \leqslant -X/2 \\ 1, & \text{if } \tau + aY + a^2 X > -X/2. \end{cases} \tag{3.6}$$

(ii) N-Wave: The solution of the incoming field in the (X', τ', Y')-variables is given by

$$P(X', \tau', Y') = \begin{cases} -\frac{\tau'}{X'+1} & , \text{ if } |\tau'| \leqslant \sqrt{(1+X')/2} \\ 0 & , \text{ otherwise} \end{cases} \tag{3.7}$$

and the solution of the incoming field in the (X, τ, Y)-variables is given by

$$P(X, \tau, Y) = \begin{cases} -\frac{\tau+aY+a^2X}{X+1} & , \text{ if } |\tau + aY + a^2X| \leqslant \sqrt{(1+X)/2} \\ 0 & , \text{ otherwise.} \end{cases} \tag{3.8}$$

(iii) Periodic Saw-tooth Wave: The solution of the incoming field in the (X', τ', Y')-variables for each period in [-1,1] is given by

$$P(X', \tau', Y') = \begin{cases} -\frac{\tau'+1}{X'+1} & , \text{ if } -1 < \tau' \leqslant 0 \\ -\frac{\tau'-1}{X'+1} & , \text{ if } \quad 0 < \tau' \leqslant 1 \end{cases} \tag{3.9}$$

and the solution of the incoming field in the (X, τ, Y)-variables for each period in [-1,1] is given by

$$P(X, \tau, Y) = \begin{cases} -\frac{(\tau+aY+a^2X+1)}{X+1} & , \text{ if } -1 < \tau + aY + a^2X \leqslant 0 \\ -\frac{(\tau+aY+a^2X-1)}{X+1} & , \text{ if } \quad 0 < \tau + aY + a^2X \leqslant 1. \end{cases} \tag{3.10}$$

We note that the above wave is of period 2 with shocks at 0,$\pm$2, $\pm$ 4, ...

We denote the computational boundary in the (τ, Y)-variables as EFGH (see figure 2). We impose the rigid boundary condition $\partial P/\partial Y$=0 on the boundary EF. Since the propagation of the shock wave is downstream, we use a backward difference for the τ variable in our finite differences scheme, which makes the boundary FG a free boundary. This allows us to minimize the complications defining the condition on the boundary GH if we choose its length large enough so that *the reflected shock does not touch the boundary GH through out the computation*, as shown in figure 2. For the transient step shock and N-wave, we further assume that *the incident shock enters the computational domain through the boundary GH* as shown in figure 2. With the above two assumptions, we can impose the solution (equation (3.6) or (3.8)) of the 1-dimensional Burgers' equation (3.4)

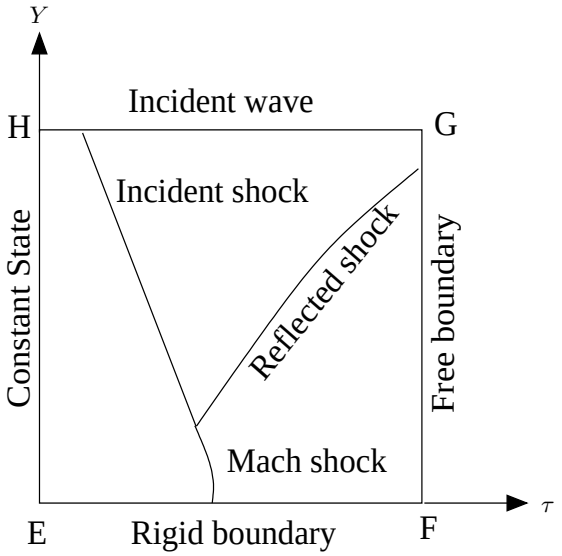

FIGURE 2. The computational domain and the boundary conditions.

on the boundary GH and a constant state (zero) on the boundary HE. For the periodic saw-tooth wave, the first assumption only is sufficient to impose the solution (3.10) of the 1-dimensional Burgers' equation (3.4) on the boundary GH, while boundaries FG and HE are handled simultaneously by the periodicity condition. The numerical algorithm used to solve the KZ-equation (2.1) in the transient case is identical to the split-step, finite differences scheme developed by Coulouvrat & Marchiano (2003) and Marchiano *et al.* (2005) to study the nonlinear diffraction of weak shock waves respectively by a screen or at a cusped caustic. The nonlinear part of the wave evolution is treated by a shock-fitting algorithm based on the exact Poisson solution and weak shock theory, so as to minimize numerical dissipation and dispersion effects and track shock waves with highest precision. The linear diffraction part is solved by the finite differences algorithm of Lee & Hamilton (1995). For the periodic case, the numerical solver is similar to the one developed by Auger & Coulouvrat (2002) and Marchiano *et al.* (2003), where time derivatives for the diffraction part are evaluated by the pseudo-spectral technique to guarantee periodicity.

The reader is referred to these references for details about the scheme, including many validation tests such as convergence of the solution with mesh refinement, comparison with analytical solutions or experimental data, and recovery of self-similar properties of solutions. Here similar tests have been performed for the case of reflection, with similar results, and are therefore not all reproduced. However, properties of self-similarity of the numerical solutions in agreement with theory are demonstrated in the next section 4 (figure 3), and perfect agreement between numerical simulations and two-shock theory in the case of nonlinear regular reflection, is also demonstrated later on (section 5, figure 10). Finally, preliminary comparison with experimental data also shows some excellent agreement with numerical simulations (see Baskar, Coulouvrat & Marchiano 2006).

4. About Self-Similarity

In this section, we discuss the similarity behaviour for the step shock, N-wave and the saw-tooth wave reflection as a solution of the KZ-equation. Self-similarity (also called pseudo-steadiness) of the step shock reflection problem on a flat rigid surface has been assumed since the pioneering work of von Neumann (1943), and then in most of the theoretical subsequent works mentioned in the introduction. First we will recover the self-similarity of the step shock problem for the KZ-equation as expected from the work of Hunter & Brio (2000) using the equivalent 2-dimensional Burgers' equation. However, we will show that this behaviour is restricted only to this ideal case, while realistic acoustical signals such as N-waves or saw-tooth waves will be proved to be not self-similar. In this case, we expect (as will be demonstrated in section 6) more complex nonlinear reflection effects similar to the unsteady reflection of the step shock over a concave double wedge (see Ben-Dor 1992). Notice that this case is different from the

nonlinear Fresnel diffraction of weak shock waves, where all the three kinds of waves exhibit self-similar behaviour (see Coulouvrat & Marchiano 2003).

We introduce the following rescaling

$$P \to P^* P,\ X \to X^* X,\ Y \to Y^* Y \text{ and } \tau \to \tau^* \tau, \tag{4.1}$$

where the quantities with superscript $*$ denote the rescaling amplitude of each corresponding variable.

The condition for the KZ-equation (2.1) to be invariant under the above rescaling is given by

$$P^* = \tau^*/X^*,\ Y^* = \sqrt{X^* \tau^*}. \tag{4.2}$$

To make the step shock (3.6) invariant, we need to choose

$$P^* = 1,\ \tau^* = X^*,\ Y^* = X^*.$$

Hence, the self-similar solution for the step shock takes the form

$$P(X, \tau, Y) = Q\left(\xi = \frac{\tau}{X},\ \eta = \frac{Y}{X}\right). \tag{4.3}$$

Substituting the above self-similar solution in the KZ-equation (2.1), we get

$$\frac{\partial Q}{\partial \xi} + \xi \frac{\partial^2 Q}{\partial^2 \xi} + \eta \frac{\partial^2 Q}{\partial \eta \partial \xi} + \frac{\partial^2 Q}{\partial^2 \eta} + \frac{1}{2} \frac{\partial^2 Q^2}{\partial^2 \xi} = 0.$$

Obviously, the incident plane wave equation (3.5) also satisfies self-similarity under the above rescaling, as does the homogeneous boundary condition on the rigid surface. It is important to notice that the self-similar solution must also satisfy the jump relation (2.6). Since, the self-similar rule in the present case is identical to the Fresnel solution discussed by Coulouvrat & Marchiano (2003), the compatibility condition for the shock curve in the self-similar coordinates can be derived identically.

We depict in figures 3a to 3c, the numerical simulation of the KZ-equation for the reflected step shock at $X = 1$, 2 and 3 respectively, rescaled in the self-similar variables.

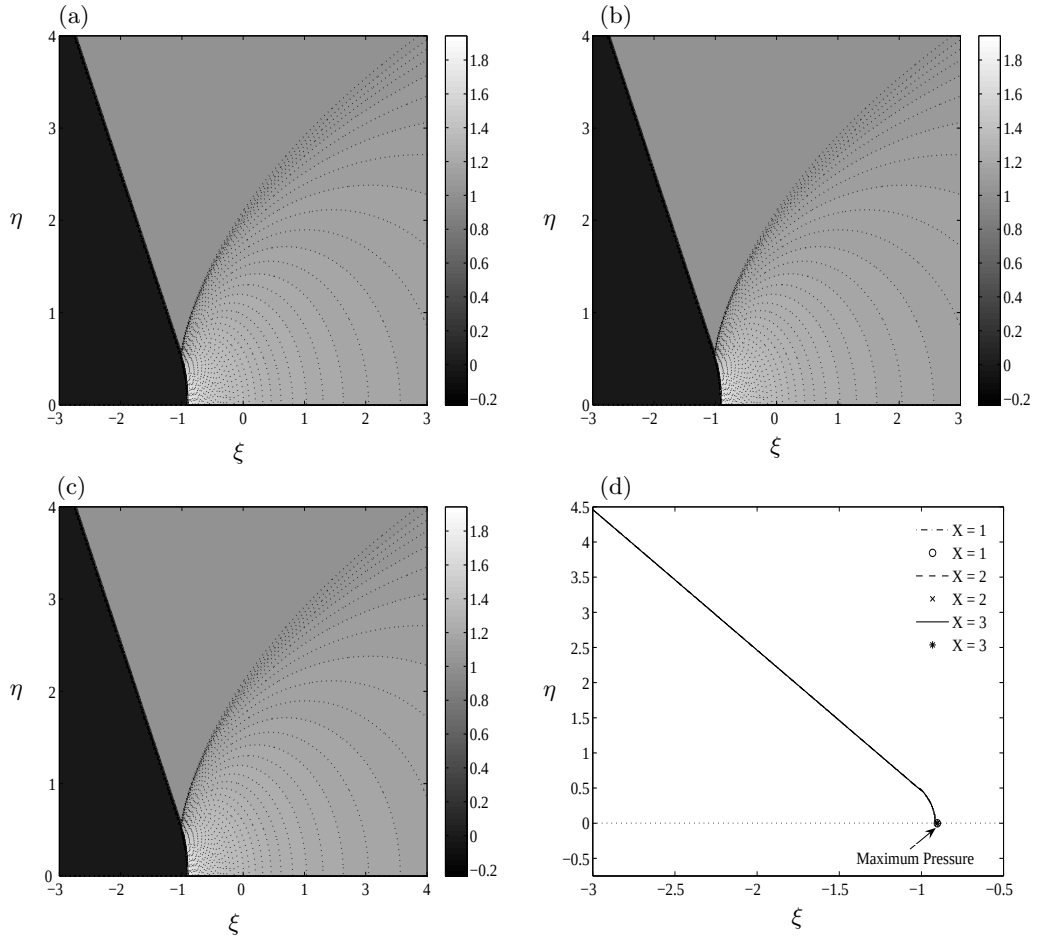

FIGURE 3. Numerical demonstration of the self-similarity property: pressure field (in gray levels) for a=0.5 and X=1.0 (a), 2.0 (b), 3.0 (c). Contour lines are dotted. Plot (d) superimposes the computed incident and Mach shock, and the positions of the maximum pressure for the same values of X. All figures are plotted in self-similar coordinates.

The comparison shows that the curves superimpose almost perfectly, which proves that the numerical simulation indeed perfectly captures the self-similar behaviour of the solution. This is confirmed by figure 3d, where the positions of the incident and Mach shock fronts, and of the points of the maximum pressure for the same three distances X are undistinguishable.

For the N-wave, to make the expression (3.8) invariant under the rescaling (4.1) with

the invariance condition (4.2) of the KZ-equation, we at least need a condition which transforms the phase of the wave from $\frac{\tau}{\tau^*}+a\frac{Y}{Y^*}+a^2\frac{X}{X^*}-\sqrt{\frac{X}{2X^*}}$ to $\tau+aY+a^2X-\sqrt{X/2}$. This is possible only in the case when $\tau^*=X^*=Y^*=1$ and therefore we cannot have a self-similar solution for the N-wave. Similarly we can prove that there is no self-similar solution for the periodic saw-tooth wave. However, in the numerical results depicted in section 6, we observed that the solutions in these two cases have almost self-similar behaviour for sufficiently small values of X, which is in fact expected from the above expression.

5. Regimes of regular and irregular reflection for step shocks

The purpose of this section is to investigate the nature of the reflection of step shocks depending on the value of the critical parameter a introduced in section 3. Reflection is mainly of two types, namely regular reflection and irregular reflection. First we will study theoretically the conditions on a for transition between these two types of reflection. Then, we will review numerically and classify the different reflection patterns by varying the critical parameter a from infinite to zero.

5.1. *Triple-point condition*

Let us consider the self-similar flow (as proved in section 4) associated to the step shock reflection. We assume that the reflected wave is a shock when it hits the incident shock. In other words, we assume that the triple point does exist and we denote its position in self-similar coordinates as (ξ^*,η^*). We consider the domain $\eta>\eta^*$ above the triple-point and assume classical Mach reflection, in the sense that the incident, reflected and Mach shocks are straight lines separating three constant states. Then the pressure field,

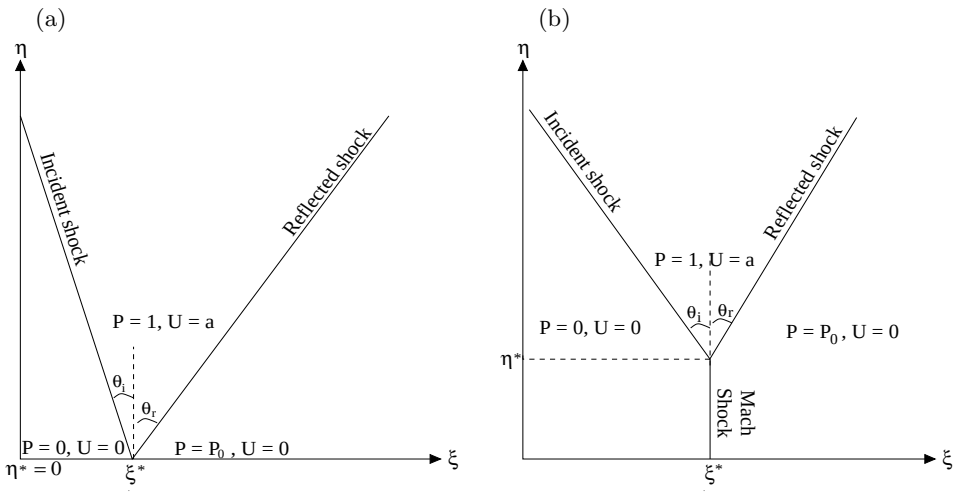

FIGURE 4. Sketch of (a) Regular reflection, (b) Mach reflection.

solution of the KZ-equation in the domain $(\xi, \eta > \eta^*)$, is given by

$$P(\xi,\eta) = \begin{cases} 0 & , \text{ if } \xi \leqslant \xi_s^i(\eta) \\ 1 & , \text{ if } \xi_s^i(\eta) < \xi \leqslant \xi_s^r(\eta), \\ P_0 & , \text{ if } \xi_s^r(\eta) < \xi \end{cases} \tag{5.1}$$

where ξ_s^i and ξ_s^r are the incident and reflected shocks respectively, which are given by

$$\xi_s^i(\eta) = -a\eta - (a^2 + 1/2) \tag{5.2}$$

for the incident shock according to the boundary condition (3.6) and

$$\xi_s^r(\eta) = b\eta - ((a+b)\eta^* + a^2 + 1/2) \tag{5.3}$$

for the reflected shock. In equation (5.3), the parameter b associated to the slope of the reflected shock is defined similarly to the parameter a as given in (3.3), but now for the reflected angle θ_r (say) instead of the incident angle (figure 4). The change of sign in equation (5.3) compared to (5.2) holds for a reflected wave and the constant is chosen so that the two shocks meet at the triple-point. In equation (5.1), P_0 is the dimensionless pressure behind the reflected shock, which is yet to be calculated. Our problem is to

find the condition on b and P_0 as a function of a, in such a way that the reflected shock satisfies the Rankine-Hugoniot condition. The triple point (ξ^*, η^*) is given by

$$\xi^* = -a\eta^* - (a^2 + 1/2). \tag{5.4}$$

The incident shock velocity $\boldsymbol{W}^i$ and the unit normal vector to the incident shock $\boldsymbol{N}^i$ are given by

$$\boldsymbol{W}^i = \left(-(a^2 + 1/2), 0\right), \ \boldsymbol{N}^i = \frac{1}{\sqrt{1+a^2}}(1, a).$$

The reflected shock velocity $\boldsymbol{W}^r$ and the unit normal vector to the reflected shock $\boldsymbol{N}^r$ are given by

$$\boldsymbol{W}^r = \left(-((a+b)\eta^* + a^2 + 1/2), 0\right), \ \boldsymbol{N}^r = \frac{1}{\sqrt{1+b^2}}(1, -b).$$

Any of the two Rankine-Hugoniot relations (2.4) or (2.5) for the incident shock gives the value $U_0 = a$. The second Rankine-Hugoniot relation (2.5) for the reflected shock gives the value $P_0 = 1 + a/b$. The first relation finally yields the relation between the incident and the reflected angles

$$(b + a)(2b^2 - 2(\eta^* + a)b + 1) = 0. \tag{5.5}$$

We note here that b should be positive, because the reflected shock has to propagate away from the surface. Thus, $b = -a$ is impossible. The other two solutions for (5.5) are

$$b = \frac{(\eta^* + a) \pm \sqrt{(\eta^* + a)^2 - 2}}{2}, \tag{5.6}$$

which results in a real value of b if and only if

$$\eta^* > \sqrt{2} - a \tag{5.7}$$

in which case both solutions are positive.

As a consequence, the triple-point reflection can exist only if the critical parameter a is smaller than $\sqrt{2}$ (so that $\eta^* > 0$). Otherwise, regular reflection must occur and the

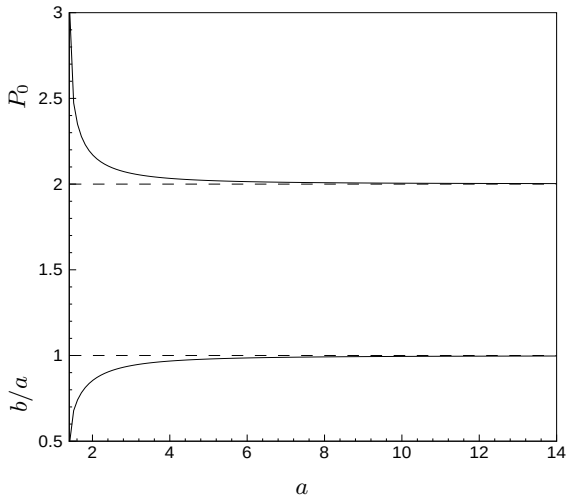

FIGURE 5. Transition from nonlinear to linear (Snell-Descartes laws) regular reflection. Upper curve : ratio of total to incident pressures. Lower curve : ratio of reflected to incident angles. The linear regular reflection occurs almost for $a > 5$.

above calculation of the reflected angle b and of the reflected pressure P_0 is valid with $\eta^* = 0$. For the regular reflection and large values of a, the positive branch of (5.6) tends towards $b = a$ and therefore $P_0 = 2$ (figure 5). Only that branch recovers the classical Snell-Descartes law for linear waves (reflected angle equal to the incident one and pressure doubling on the surface) and is consequently physically admissible. Note however that a significant deviation from the Snell-Descartes law occurs for values of a smaller than about 5. For typical sonic booms or ultrasound in water ($M = 10^{-3}$) this corresponds to angles smaller than 12 degrees. Hence, nonlinear effects will occur even for non-grazing incidences. They will appear as a reflected wave less grazing than the incident one ($b > a$), and a reflected pressure larger than the incident one ($P_0 > 2$). At the critical value where the largest deviation occurs $a = \sqrt{2}$, the pressure triples on the surface, while the reflected angle is only half the incident one.

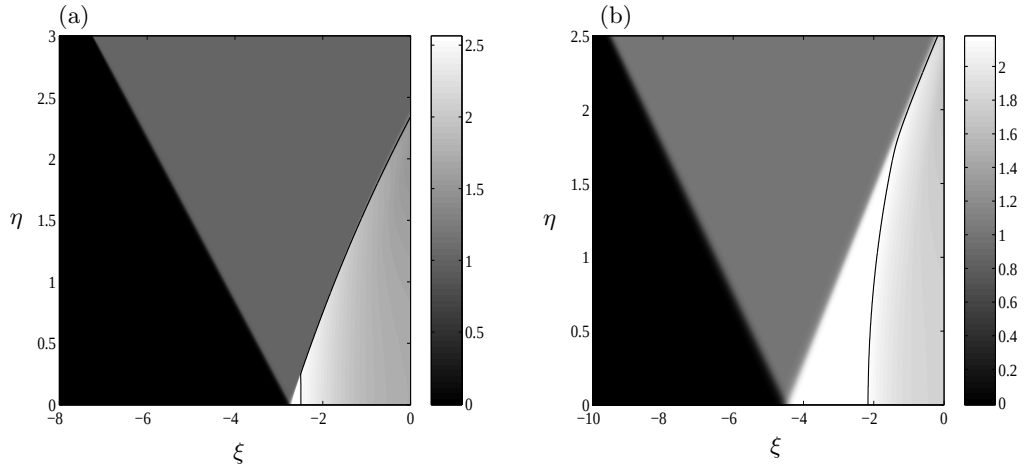

FIGURE 6. Regular reflection: Pressure field (in gray levels) in self-similar variables for a=1.5 (a) and a=2.0 (b) at X=1.0. The solid line is the sonic line.

5.2. *Regular reflection*

The relation between a and b in the above discussion shows that the nonlinearity plays a role in the regular reflection for a moderate value of a (in practice less than 5). This is illustrated in the numerical simulations for $a = 1.5$ and 2.0, which are displayed in figure 6. Obviously, on the figure, the slope of the incident and the reflected shocks in the neighbourhood of the surface are different and the pressure behind the reflected shock is greater than 2. For $a = 1.5$ in figure 6a, the numerical value of the maximum pressure, which is obtained at the reflection point is 2.5655. From (5.6), we get $b = 1$ and consequently the pressure behind the reflected shock $P_0 = 1 + a/b = 2.5$, which is very close to the numerically obtained maximum pressure. Similarly, for $a = 2$ in figure 6b, the numerical value of the maximum pressure is 2.1821 whereas the theoretical value is 2.1716. Good agreement between theoretical and numerical values will be further illustrated by figure 10 in section 5.3.

The theory detailed in section 5.1 is indeed equivalent to the von Neumann (1943) two-shock theory but restricted to the approximate KZ-equation. According to the ap-

proximations of the theory, shocks are assumed to be perfectly straight and separate only states with constant pressure and velocity. However, it is observed in the simulations that these assumptions are valid only in the vicinity of the reflection point. The physical reason for this is the existence of the wave diffracted due to the impact of the incident shock at the edge $X = 0$ of the rigid surface. This diffracted wave (neglected in the simplified theory of von Neumann) called corner signal by Henderson (1987) must have a spherically shaped wavefront (at least in linear acoustics) according to Huygens principle ; however, because of the parabolic approximation of the KZ-equation, the diffracted wavefront here has a parabolic shape. Once the diffracted wave and the reflected shock interact, the reflected shock bends and is now called diffracted shock. Consequently, the pressure field cannot be constant anymore behind it. This behaviour is very visible on figure 6b, where we can very clearly see the constant pressure state just behind the reflected shock until the arrival of the diffracted (or corner) wave with parabolic wavefront. Then, the reflected shock begins to bend and the pressure smoothly decays. Because of the self-similarity of the solution, a point with fixed τ and Y but increasingly large X in physical variables, will correspond in self-similar variables to the vanishing of ξ and η variables. Therefore, very far from the edge of the reflector, the diffracted wave lags very far behind the reflected wave. Ultimately, as $X \to \infty$ the reflected and diffracted fields will be fully separated, and the observer will see only the vicinity of the reflection point where the shocks are straight and the pressure level is constant. This limit case is simply the one described by von Neumann two-shocks theory for which the influence of the diffracted wave is discarded. In the linear regime of course, and in that farfield limit, we would recover the Snell-Descartes reflection on an infinite rigid plate.

Finally, it has to be noted that, for the Euler equations, the slope of the diffracted shock may vanish and then becomes negative so that it may propagate backward and hit

the rigid surface as sketched in figure 1 drawn according to Ben-Dor (1992). However, this inversion of the slope cannot be obtained using KZ-equation, because the paraxial/parabolic approximation prohibits any backward propagation.

The critical value denoted by $a_d = \sqrt{2}$ obtained in section 5.1 near which the transition from the regular to irregular reflection takes place is called the *deflection point* (see Hunter 1991). Another transition condition called *sonic point* is obtained using the notion of sonic line. The system (2.2)-(2.3) in the self-similar variables (ξ, η) is given by

$$(\xi + P)\frac{\partial P}{\partial \xi} + \eta\frac{\partial P}{\partial \eta} + \frac{\partial U}{\partial \eta} = 0, \tag{5.8}$$

$$-\frac{\partial U}{\partial \xi} + \frac{\partial P}{\partial \eta} = 0. \tag{5.9}$$

The eigenvalues of the above quasi-linear system are $\left(\eta \pm \sqrt{\eta^2 - 4(\xi + P)}\right)/2(\xi + P)$, which shows that the system (5.8)-(5.9) changes its nature from hyperbolic to elliptic across the parabola

$$\frac{\eta^2}{4} - \xi = P. \tag{5.10}$$

The curve $\eta = 2\sqrt{\xi + P}$ is called the *sonic line*. The positive side of the parabola is the elliptic region and the negative side is the hyperbolic region. The sonic lines is plotted along with each of the numerical solutions for a=1.5 and 2 on figure 6. Note that the sonic line on figure 6b is extremely close to the diffracted wave beyond which the pressure ceases to be constant. Also, visible on the figure is the identification of the sonic line with the curved part of the reflected shock. The notion of sonic line allows to derive a second transition criteria between regular and irregular reflection. Indeed, the expression (5.10) shows that the reflection point $(\xi^*, 0)$ lies in the hyperbolic region if and only if

$$-P_0 > \xi^*, \tag{5.11}$$

where P_0 is the pressure at the reflected point, which is the maximum pressure in the entire pressure field as shown in figure 3d.

For regular reflection, the reflection point is given by $(-(a^2+1/2), 0)$ (see equation (5.4)). From (5.6) and $P_0 = 1 + a/b$, we have

$$P_0 = a^2 - a\sqrt{a^2-2} + 1. \tag{5.12}$$

Thus, the reflection point lies in the hyperbolic region if and only if

$$a^2 - a\sqrt{a^2-2} + 1 < (a^2 + 1/2),$$

which implies

$$a > \sqrt{1+\sqrt{5}/2} = a_s.$$

It is well known that a shock cannot appear in an elliptic region. Thus, for the regular reflection, the reflection point has to lie in the hyperbolic region. The constant a_s is the transition condition in the sense that for $a < a_s$, the regular reflection cannot exist. The constant a_s=1.4553 is the sonic point at which the reflection point lies right on the sonic line. The values a_s and a_d obtained here are the same as those derived by Brio & Hunter (1992). Note that the detachment constant $a_d = 1.4142$ is very close to the sonic point a_s. Because of this reason, these two transition conditions are usually considered as equivalent in the literature (see Colella & Henderson 1990), though the reflection pattern between these two extremely close values remains to be explorated. Note that a third transition condition called *Crocco point* based on the condition that the stream lines behind the reflected shock are approximately straight, can also be derived (see Brio & Hunter 1992) and yields an intermediate value $a = 1.4278$.

5.3. *Irregular reflection*

In section 5.1, we have proved that for $a < \sqrt{2}$, the regular reflection ceases to exist. Indeed from the triple-point condition (5.7), we necessarily have $\eta^* > 0$, which implies that the reflected wave (here we use the word wave instead of shock as we will see in this

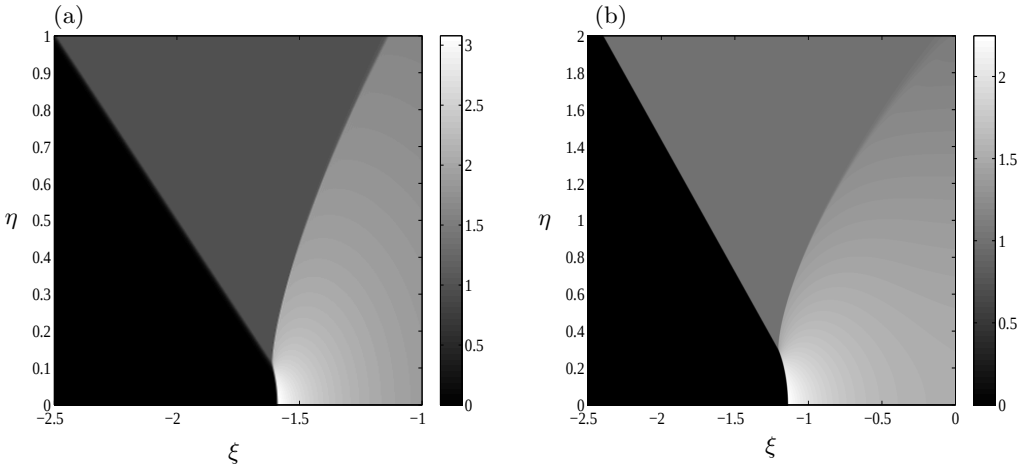

FIGURE 7. Von Neumann reflection: Pressure field (in gray levels) in self-similar variables for a=1.0 (a) and a=0.7 (b) at X=1.0.

section that it is not necessary that the reflected wave is always a shock when it intersects the incident shock) intersects the incident shock above the rigid surface, a pattern known as irregular reflection. More precisely we will show that there are two different types of irregular reflection observed in our numerical results, which we discuss in this subsection depending on the value of the critical parameter a between $\sqrt{2}$ and 0.

The first regime is observed for values of a between about 0.4 and $\sqrt{2}$. Figure 7 (a and b) depicts the reflection solution for $a = 1.0$ and 0.7, respectively. In this regime we can clearly see three shocks, namely the incident shock, the reflected shock and the Mach shock. These three shocks meet at the point T called *triple point*. While the incident shock is straight, the Mach and the reflected shocks are obviously curved, contrarily to the classical Mach reflection. Also the classical definition of Mach reflection (see Ben-Dor 1992) implies the presence of a slipstream (discontinuity of the entropy, density, temperature and tangential velocity component) attached to the triple point. Such a slipstream cannot exist in the KZ-equation associated to weak amplitude approximation, because temperature and density fluctuations are proportional to pressure ones, while

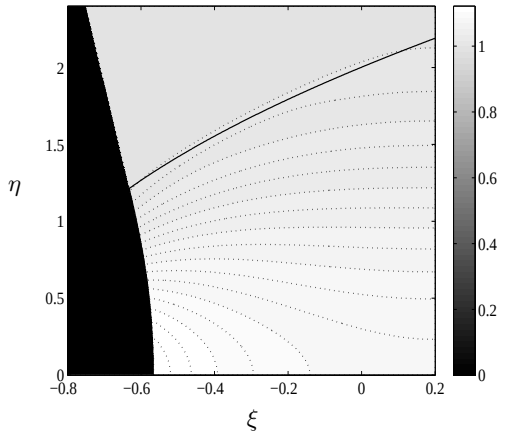

FIGURE 8. Weak von Neumann reflection: Pressure field (in gray levels) in the self-similar variables for a=0.1 and X=1. Contour lines are dotted and sonic line is solid.

entropy discontinuity is of third order and therefore is neglected. Finally, classical Mach reflection occurs for a moderately strong shock (see Henderson 1987 for more discussion on weak and strong shocks). As outlined in the introduction, the question of existence of a triple shock for weak shocks (and therefore for the KZ-equation or its equivalent 2-dimensional Burgers' equation) remains controversial. We refer the reader to the cited references for the proposed solutions for the classical von Neumann paradox. Again, we recall the objective of the present work is not to investigate this well studied phenomenon, but to study the transition between the different regimes in the acoustical case, therefore to solve the acoustical von Neumann paradox (see the introduction for the definition). So we will label the present regime *von Neumann reflection* according to the terminology most frequently used in the literature, and this independantly of the exact behaviour of the solution near the triple point.

For smaller values of parameter a, the reflected shock progressively weakens up to complete disappearance. This is illustrated by figure 8 representing the pressure field at value $a = 0.1$. Here obviously the reflected wave field is simply a smooth compression

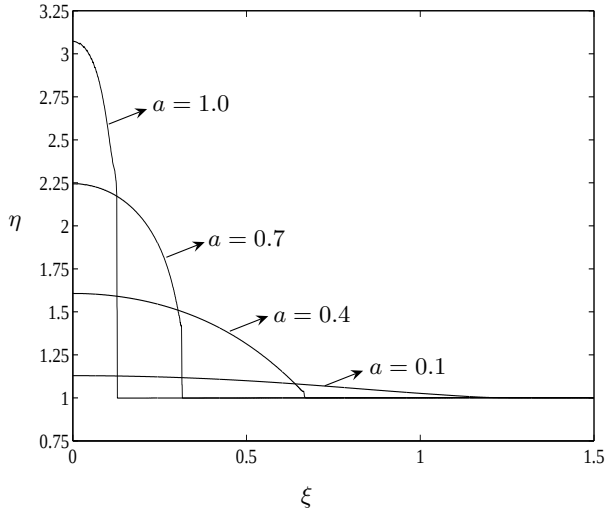

FIGURE 9. Pressure amplitude just behind (5 grid points) the incident and Mach shocks at X=1 and a=0.1-1.0 with step 0.3. Both the maximum pressure amplitude (obtained on the rigid surface) and the shock strength increase with increasing a. The strength of the shock is very small for $a = 0.4$ around which the transition from von Neumann to weak von Neumann reflection is expected to take place. The profile for $a = 0.1$ is smooth.

wave ahead of the incident shock. The smaller the value of the parameter a, the weaker this wave will be, up to complete disappearance for $a = 0$. This reflection regime with no reflected shock at all has never been observed to our knowledge. This regime is completely opposite to the Snell-Descartes linear regime. In this last one, the whole pressure field is completely in the hyperbolic domain, with a perfectly straight reflected shock and a sonic line pushed away at infinite. On the contrary, in the present regime, there is no reflected shock and almost all the reflected pressure field lies in the elliptic domain as is visible in figure 8 where the sonic line has been drawn. Note however that an extremely small part of the reflected wave lies in the hyperbolic region. The question therefore arises whether there exists a reflected shock of very small amplitude as hypothesized by Hunter & Brio (2000). Our numerical simulations show that, whatever the grid refinement of the numerical domain (up to 5 times more than the one used for figure 8), there is absolutely

no change in the numerical solution which remains continuous. So, we believe that for small values of the parameter a, no reflected shock does exist.

We label this new regime *weak von Neumann reflection* in reference of the paragraph of von Neumann (1943), where he raises the problem of the acoustical limit. The transition between von Neumann and weak von Neumann reflection is illustrated by figure 9, which shows the pressure variation along (just behind) the incident and Mach shocks for $a =$ 0.1 to 1.0. We clearly observe the existence of a pressure jump (down to the constant value 1) associated to the triple point for the values of a greater than or equal to 0.4. On the contrary, for the smaller values (for clarity, only the value $a = 0.1$ is displayed, but it has been checked also for a=0.2 and 0.3) the curves are continuous, thus indicating there is no reflected shock in direct contact with the incident one. From the numerical results, it can also be observed that the arc length of the Mach shock decreases as the value of a increases, which eventually results into a regular reflection for a sufficiently large value of $a(\geqslant \sqrt{2})$ as already discussed in section 5.1 and 5.2.

As recalled in the introduction, von Neumann remarked that the transition from the well known Snell-Descartes laws to the vanishing reflected wave (for $a = 0$) is singular, in the sense that the former is valid at any grazing angle except the zero angle, where there cannot be any reflected wave. This singular transition was stated as an acoustical paradox by von Neumann. In his original paper, von Neumann expects a different behaviour for extremely weak acoustical shock waves, and for other stronger shocks. In the acoustical case, he expects a monotonic decrease of the reflected amplitude with grazing, while he describes a more complex pattern in the other case. Our present study proves on the contrary that there is no fundamental difference between an acoustical shock wave and other stronger shocks. This is illustrated by figure 10, which summarizes the different regimes of reflection observed above, by plotting the (dimensionless) maximum total pressure as

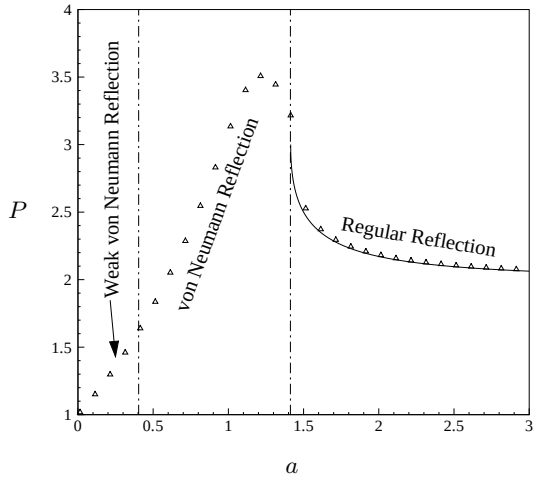

FIGURE 10. Solution of von Neumann acoustical paradox illustrated by maximum overpressure as a function of the critical parameter a: the transition from Snell-Descartes to perfectly grazing incidence involves successively regular, von Neumann and weak von Neumann reflections. Solid line is the weak two-shock theory and symbols $\triangle$ are numerical computations.

a function of the parameter a (or equivalently as a function of the grazing angle for an incident shock wave of fixed amplitude). Obviously, though we are dealing here only with weak acoustical shocks, the transition from linear Snell-Descartes laws (value of 2 for high values of the parameter a) to the perfectly grazing case (value of 1), is not monotonic. When decreasing the value of parameter a, we observe an increase of the pressure, first according to the regular reflection law (continuous line for equation (5.12)). Below the critical value $a = \sqrt{2}$, the increase keeps on, now in the von Neumann reflection regime. The maximum, about 3.5 times the incident amplitude, is reached slightly below the critical value, at about $a = 1.2$. It is only below this value, that a monotonic behaviour is finally observed. Keeping on decreasing the parameter a, the maximum pressure falls down progressively, entering finally the weak von Neumann regime around $a = 0.4$. Note also that the number of shocks involved in the reflection varies from two (regular reflection) to three (weak Mach reflection) and finally to one (weak von Neumann reflection).

Of course, for a very small shock amplitude, this complex transition will occur only over an extremely small range of grazing angles (in practice a few degrees). It may be difficult to observe, and this all the more as other competing effects than nonlinearities may affect the process, such as viscosity, thermal effects, surface roughness, curvature and elasticity. However, this nonlinear non-monotonic behaviour has been observed experimentally for ultrasonic shock waves produced in water (see Baskar, Coulouvrat & Marchiano 2006). So, we can conclude here that the two extreme linear regimes (perfectly grazing and Snell-Descartes) can indeed be matched continuously as expected by von Neumann, but this matching is unexpectedly inherently nonlinear and non-monotonic.

6. Unsteady reflection of N-waves and saw-tooth waves

The discussion in section 5 has shown that the reflection of a weak amplitude step shock can lead to different regimes of reflection. However, step shocks are not very realistic for acoustical waves and the question remains open for the reflection regimes of more complex but physically relevant wave profiles. This is the objective of the present section, to investigate whether irregular reflections also occur for realistic acoustical waves. We have selected the case of N-waves (section 6.1) and periodic saw-tooth waves (section 6.2).

6.1. *N-waves*

We consider the incident shock to be an N-wave as defined in (3.8). Unlike the step shock discussed in section 5 we have here two shocks, the leading shock with a compression from the ambient state and the rear shock with a recompression back to the ambient state, the two being connected by an expansion wave. When the leading shock encounters the wedge surface, the reflection takes place. As a consequence the associated reflected wave interacts nonlinearly with the expansion wave, and will thus affect the reflection of the

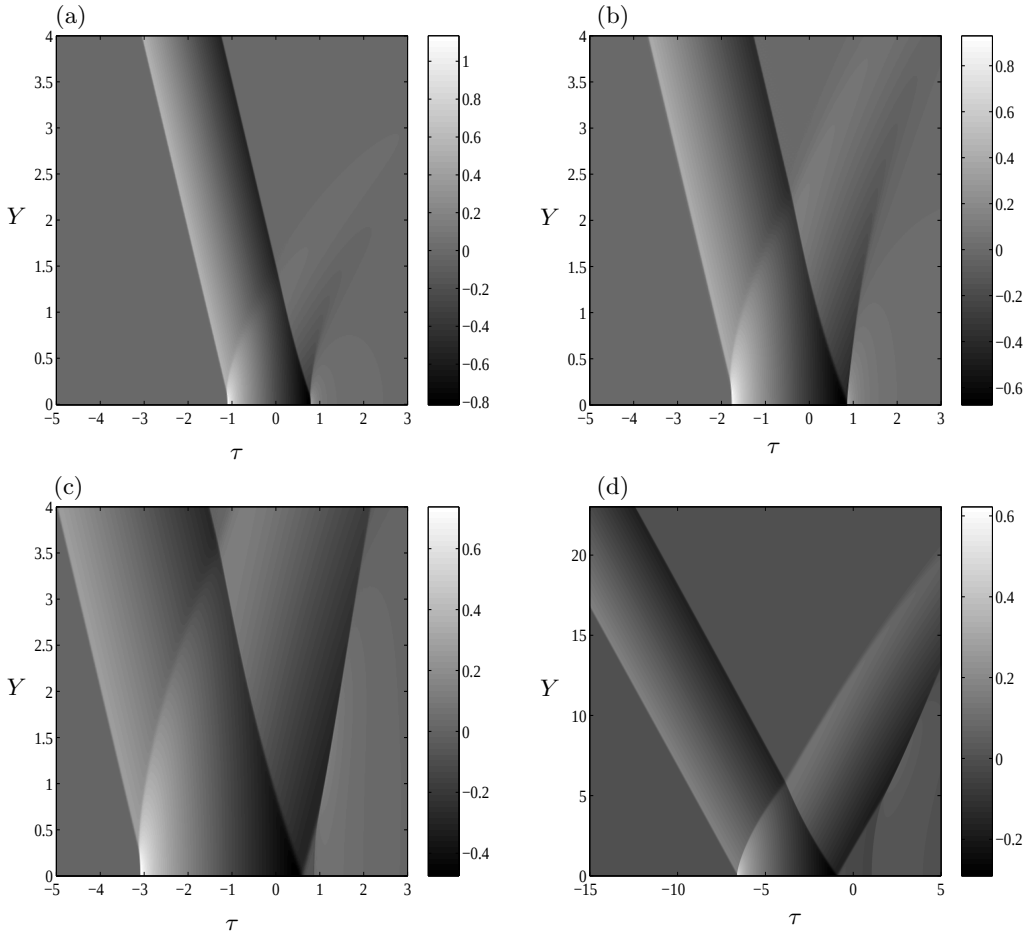

FIGURE 11. Unsteady irregular reflection of an N-wave: Pressure field (in gray levels) as a function of the (τ, Y) variables for $a = 0.5$ at X=0.603 (a), 1.8593 (b), 5.0 (c) and 15.0 (d).

rear shock. This interaction is an additional phenomenon compared to the simplified step shock case.

Figure 11 (a)-(d) depicts the reflection solution for $a = 0.5$ (a value chosen for being representative of irregular reflection in the step shock case) and for different values of the distance $X = 0.603$, 1.8593, 5 and 15 from the edge of the plate respectively, covering a sufficiently long propagation distance. In figure 11 (a), we obviously observe the irregular (von Neumann type) reflection of both the leading and the rear shocks. At such small values of X, the main difference with the step shock case is the fact that the incident

rear shock is slightly curved because of the interaction with the reflected wave. If we decrease the value of the parameter a, we observe also, as for the step shock, the weak von Neumann reflection around $a = 0.4$ (figure not shown here) for sufficiently small values of X. This indicates (as remarked at the end of section 4) that near the tip of the plate, the reflection of the N-wave is similar to the step shock case. However, because the N-wave case is not self-similar (as proved in section 4), this cannot last all along the propagation.

From equation (3.8), we see that the incident shock amplitude decreases with distance as $O(1/\sqrt{X})$. This decrease results in an increase of the local "true" value of the parameter a and therefore tends to decrease the length of the Mach stem. This effect competes with the tendency of the Mach stem to increase in length as for a step shock because of self-similarity. Therefore, for an N-wave, we initially observe a behaviour similar to step shocks with an increase of the length of the Mach stem. This is named *direct irregular reflection*. As the pressure amplitude decreases, as is visible by comparing the length of the Mach stem between figures 11a and 11b or 11c, it then reaches a maximum before progressively decreasing, a regime named *inverse irregular reflection*. Finally, when the triple point touches the rigid surface at a finite X value called *termination point*, the irregular reflection is replaced by the regular reflection. This final reflection regime for the head shock is observed in figure 11d. A similar behaviour will be detailed in section 6.3 for periodic saw-tooth wave. From the above discussion we see that there are two types of irregular reflection configuration that take place for the leading shock. Courant & Friedrichs (1948) have categorized these two reflections for the step shock and the names of direct or inverse irregular reflection and termination point were suggested by them.

It has also been observed from our numerical experiments that the value of the ter-

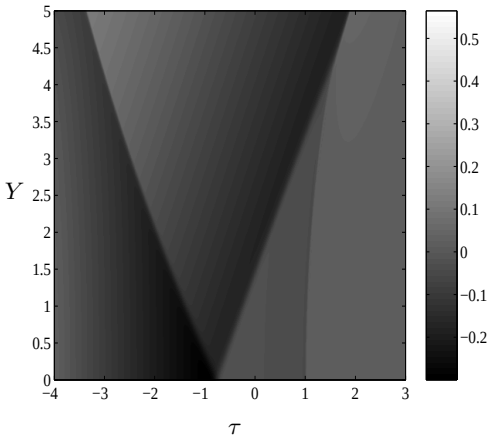

FIGURE 12. Transitioned regular reflection of type 2: closer view (pressure field in gray levels) of the rear shock for a=0.5 at X=15.0.

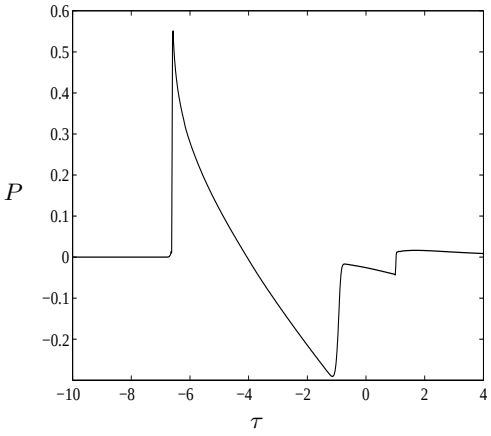

FIGURE 13. Pressure time waveform on the rigid surface for $a = 0.5$ at $X = 15.0$, which clearly shows the presence of the secondary reflected shock.

mination point and the maximum of the triple point trajectory both decrease as the value of a increases, as logically expected as we are closer to regular reflection. Thus, for a sufficiently large value of a, which is observed approximately as 0.8, there is no irregular reflection at all, the head shock reflecting always regularly all along the plate. Thus, with this study, we categorize the types of reflection for the leading shock as the regular reflection (approximately for a greater than 0.8), *dynamical irregular reflection* (approximately for $0.4< a < 0.8$) and weak reflection (approximately for $a < 0.4$), where initially the reflected wave is not a shock. The exact transition condition between these three types of reflections and the presence of any further types of irregular reflection are yet to be investigated. Note however that this categorization is different from the step shock case where it remains valid all along the plate because of self-similarity. Here, because of the incident wave amplitude decay, the reflection process is now dynamical. Whatever the regime it begins with, it always converges towards the regular reflection and ultimately towards the linear Snell-Descartes laws.

The reflection phenomena for the rear shock of the N-wave is somewhat different from the leading shock discussed above. Initially we observe the same succession of direct and inverse irregular reflections, with the only difference that the length of the Mach stem remains smaller than the head shock (though the shocks are of same amplitude). The inverse irregular reflection terminates when the triple point hits the rigid surface. The difference between the leading and the rear shocks occurs after the termination. Indeed for the rear shock, we observe an additional shock, which is called *secondary reflected shock*, that detaches from the reflected shock right at the termination point. Our interpretation is that this new shock emerges from the impact on the rigid surface of the reflected shock when this one collides with the surface at the termination point. This new kind of reflection therefore has to create a new reflected shock, which appears as a secondary reflected shock. For this secondary reflection pattern, the primary reflected shock plays the role of the incident shock, the secondary reflected shock plays the role of the reflected shock and the two merge into a single reflected shock, that plays the role of the Mach shock, at a new, *secondary triple point*. The only difference with the classical weak Mach reflection is now that the Mach shock extends away from the surface. This reflection pattern is visible on figure 11 c and d. A closer view is provided by figure 12 where the four shocks are visible (incident rear shock, primary reflected shock, secondary reflected shock and the merging of the two last ones into a Mach shock). Figure 13 displays the pressure time profile for $a = 0.5$ and $X = 15$ on the rigid surface where we can clearly observe this new secondary reflected shock at the trailing part of the wave profile. This secondary reflection appears absolutely similar to the von Neumann reflection described in section 5. Indeed, we can observe from figure 11d and 12 that here the primary reflected shock (playing here the role of an incident shock) seems almost straight, the Mach shock is slightly curved while the secondary reflected shock has to

be strongly curved to match the inclination of the secondary Mach shock at one end and the normal boundary condition on the surface at the other end. Finally, for long distances, the terminated reflection of the incident rear shock remains regular (we expect it to fit linear Snell-Descartes law at very large distance where the amplitude will be small). Because of this nature of the terminated reflection, this type of reflection is called transitioned regular reflection of *type 2*.

The transitioned regular reflection of type 2 has been described by Takayama & Ben-Dor (1985) for step shocks reflection on a concave rigid surface. Here the curvature of the surface has been replaced by a decrease of the amplitude of the incident wave, but both are similar in the sense that the local critical parameter a is not constant but increases along the reflecting surface. Also, it is similar because in both cases (step shock reflection on a concave surface, or reflection of a decreasing amplitude wave along a plane surface) the ambient state behind the incident shock is constant. This is not the case for the leading shock of the N-wave, for which this type of transitioned regular reflection is not observed, with no secondary reflected shock. The transitioned regular reflection observed for the leading shock of the N-wave is therefore called of *type 1*, to distinguish it from the type 2, the one observed for rear shock. We will see in the next subsections, that the type 1 reflection is also observed for the periodic saw-tooth wave.

6.2. *Periodic Saw-tooth Wave*

Finally, we consider the incident shock to be a periodic saw-tooth wave as given in (3.10), with the objective of investigating the interactions between the successive incident and reflected shocks. Figure 14 shows the propagation of the periodic saw-tooth wave for $a = 0.5$ at different distances. As for the N-wave, we observe the existence of an unsteady irregular reflection due to the competition between nonlinear effects at grazing angle and the decrease of the amplitude. This results in a direct and then inverse irregular

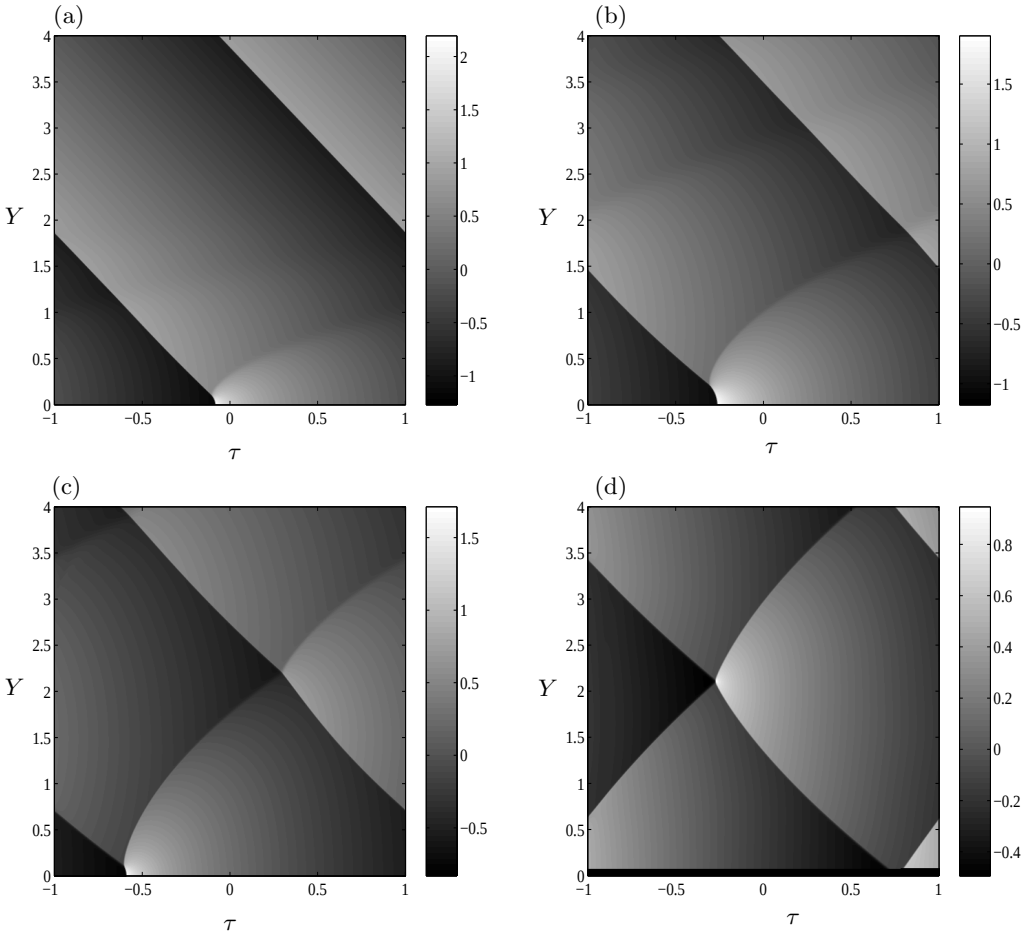

FIGURE 14. Unsteady irregular reflection of the periodic saw-tooth wave: pressure field (in gray levels) in (τ, Y) coordinates for $a = 0.5$ at X=0.2462 (a), 1.0 (b), 2.5075 (c) and 5.0201 (d).

reflection, up to termination and return to the regular reflection. The trajectory of the triple point is illustrated on figure 15 for $a = 0.5$ and $a = 0.8$. The maximum of the length of the Mach stem is obtained at almost $X = 1$ for $a = 0.5$ and almost $X = 0.3$ for $a = 0.8$, with a rather rapid (almost linear as for the self-similar step shock case) increase during the direct phase for small X, and then a slower decrease up to X about 4.5 for $a = 0.5$ and up to X about 1 for $a = 0.8$ (the termination point is not so clearly traced from our numerical result because of the numerical diffusion near the surface). It is noticeable that the position of the termination point is highly variable with the pressure

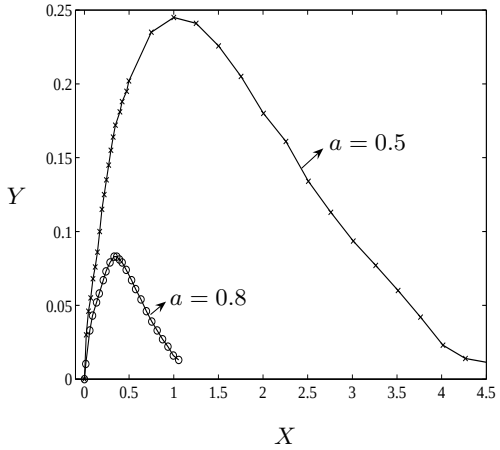

FIGURE 15. Numerically traced triple point trajectory of the saw-tooth wave for a=0.5 (with solid line and symbol $\times$) and a=0.8 (with solid line and symbol o).

waveform, with a value of about 15 for the leading shock of the N-wave and only 1.8 for the rear shock of the N-wave (for $a = 0.5$). However, qualitatively the nature of the triple point trajectories are similar to the one studied by Ben-Dor & Takayama (1985) experimentally for a step shock grazing over a cylindrical concave surface. Beyond the termination point, the reflection phenomena is a transitioned regular reflection of type 1, with no secondary reflection (the solution has been computed up to $X = 8$ without observing any secondary shock). In that sense, it is very similar to the leading shock of the N-wave. Once again, we think that this is due to the fact that the incident pressure field behind the shock is not constant (here because of the periodic nature of the wave), which seems to prevent any secondary reflection. Finally, it is to be noticed on figure 11d that beyond the termination point, the maximum amplitude of the whole pressure field does not lie anymore on the surface, but now at the intersection between the reflected shock and the next incident one. Clearly visible also is the curvature of the incident shocks due to the interaction with the reflected wave.

For transient nonlinear acoustical waves of finite energy, because shock waves are

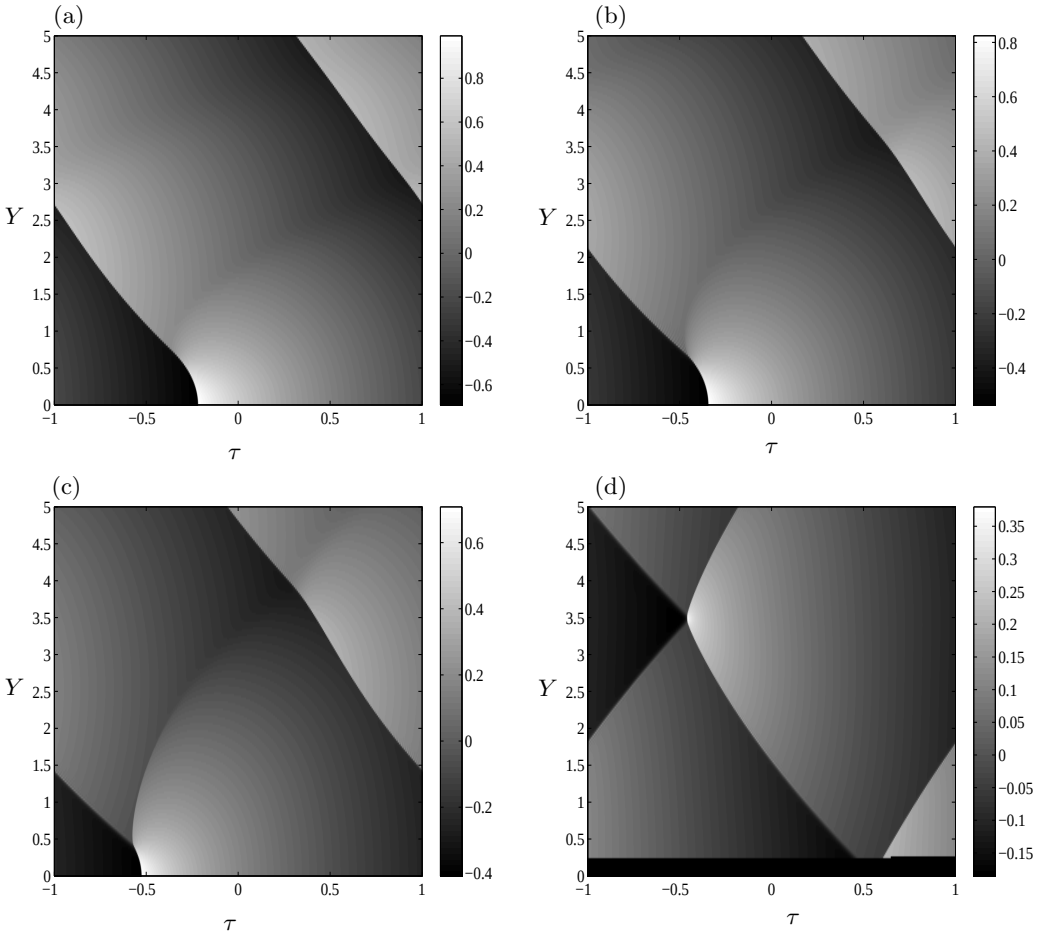

FIGURE 16. Unsteady irregular reflection of the periodic saw-tooth wave: pressure field (in gray levels) in (τ, Y) coordinates for $a = 0.3$ at X=2.0040 (a), 3.6072 (b), 6.0120 (c) and 16.0321 (d).

dissipative processes, energy decreases. As a consequence, contrarily to step shocks, the reflection phenomena cannot be self-similar, it is necessarily unsteady along the reflector and it will unavoidably converge towards regular reflection and finally to linear Snell-Descartes reflection. This has already been observed above with the transition process from Mach to regular reflection for the N-wave and the saw-tooth wave. This is also true if we initiate the process with weak von Neumann reflection as illustrated on figure 16 for a saw-tooth wave with $a = 0.3$. The computation at different distances clearly shows the transition from the weak von Neumann reflection for small X values (figure 16a with X

= 2.0) to von Neumann reflection for intermediate X values (figure 16c with $X = 6.0$), the transition occurring around $X = 3.6$ (figure 16b). Finally, for very large distances the reflection ultimately evolves into regular reflection (figure 16d with $X = 16.03$). Note here again that the maximum amplitude is not observed anymore on the surface.

So, for realistic waveforms, even for fixed incidence angle, no single reflection regime can be observed, the loss of energy of the incident wave will necessarily imply the transition from weak von Neumann to Mach to regular and finally to Snell-Descartes reflections. This transient behaviour may explain why these nonlinear reflection regimes have not been observed for acoustical shock waves up to very recently (see Baskar, Coulouvrat & Marchiano 2006).

7. Conclusion

Obliquely grazing shock wave reflection over a rigid surface is studied from the acoustical point of view. Three types of incident waves are considered, namely the step shock, the N-wave and the periodic saw-tooth wave. The shock amplitude and the grazing angle are assumed to be very weak and in a ratio (measured by the critical parameter a) ensuring the proper balance between the nonlinear and diffraction effects. This critical parameter is the key parameter of the problem in the sense that it categorizes the nature of the reflection. Though nonrealistic from an acoustical view point because it is of infinite energy, the step shock case is studied first precisely for the purpose of categorization of the reflection regimes, based on the self-similar property of the problem. Four different types of reflection ranging from very strong to very weak reflection are observed and their transition are studied both theoretically and numerically. The classical linear Snell-Descartes reflection takes place only for relatively large values of the critical parameter $a > 5$. Snell-Descartes laws are generalized (according to the weak shock theory) to the

nonlinear regular reflection for smaller values of a, but larger than $\sqrt{2}$. Regular reflection is characterized by a reflection angle and a reflected pressure amplitude larger than the incident ones. A transition condition from regular to irregular reflection is obtained theoretically at $a = \sqrt{2}$, which is the classical detachment point obtained by Brio & Hunter (1992) (another transition condition almost equivalent and called sonic condition could also be recovered). We categorize the irregular reflection into two types. The first one is the von Neumann reflection, observed for $0.4 \leqslant a < \sqrt{2}$ with the existence of the triple point. As we further decrease the value of a, we observe the complete disappearance of the reflected shock, the reflected wave being only a small amplitude, smooth compression wave. We suggest to name this new type of reflection *weak von Neumann reflection*. This continuous transition between these four regimes provides a nonlinear solution to the *acoustical von Neumann paradox* according to which the Snell-Descartes laws are singular. However, contrarily to von Neumann conjecture, that transition is not monotonic. For instance, the maximum total pressure is about 3.5 around $a = 1.2$ for the intermediate von Neumann regime, much larger than the two extreme values of two (Snell-Descartes at $a = \infty$) and one (perfectly grazing shock at $a = 0$).

For the acoustically more realistic cases of an N-wave or a periodic saw-tooth wave, the step shock categorization remains valid. However, the key difference is that the process is now unsteady because of the energy loss of the incident shock. Indeed for a given initial value of the critical parameter, the reflection patterns all along the plate will evolve from the initial one (whatever it is) to the regular reflection regime and ultimately to the linear Snell-Descartes limit. For instance, beginning with the weak von Neumann regime at the tip of the plate, we will successively observe the transitions to the von Neumann reflection and then to the regular reflection. We therefore recover types of transition similar to those categorized in the literature in the case of step shock reflecting over a concave surface.

Here the role of the surface curvature is simply replaced by the amplitude decay of the incident wave. Especially, we recover what we call type 2 transitioned regular reflection, in which a secondary reflection takes place. However, this is observed only for the rear shock of the N-wave while for all other cases (leading shock of the N-wave or periodic saw-tooth wave), this transition is only of type 1 with no secondary reflection. This kind of transition (type 1) has never been described before according to our knowledge. We assume it is due to the fact that the incident flow behind the incident shock is not constant, which seems to prevent the type 2 transition. As a consequence, this last one seems to be rather exceptional.

The present study has been restricted to a rather idealized situation despite the fact that the incident signals are more complex than the step shock. Indeed, for acoustical applications it would be necessary to take into account several effects that have been neglected here. Surface curvature would compete with amplitude decay. For a concave surface, as for the step shock situation described in the literature, we expect the curvature to accelerate the transition to regular reflection. On the contrary, a convex surface would slow down this transition and we may imagine a special surface design that would exactly compensate nonlinear attenuation. Surface roughness is also expected to significantly affect the process with hysteretical effects, as already studied for step shock (see Ben-Dor 1992). Finally, probably the most significant effect will come out from the surface elasticity. Indeed, it is well known that, for a grazing incident wave in a fluid over an elastic medium with a transverse wave speed larger than the sound speed (the common case for metallic materials), total reflection takes place with a reflection coefficient approaching -1 instead of +1 for a rigid reflector. So, we therefore expect this case to be closer to the reflection over a pressure release interface. However, pressure release reflection of shock waves produces inverted shocks that violate the second law of thermodynamics, and that

will immediately break into expansion fans. Therefore, however rigid the reflector, we expect dramatic differences with the present ideal rigid case.

The first author benefited a post-doctoral fellowship from the Ministère Délégué à la Recherche, France (décision 140, 2004). The authors are grateful to Dr. Jean-Louis Thomas (Centre National de la Recherche Scientifique UMR 7855, Institut des Nano-Sciences de Paris, Université Pierre et Marie Curie - Paris 6) for his valuable suggestions. The anonymous reviewers should be thanked for their helpful comments and suggestions about the bibliography of the present work.

REFERENCES

Auger, T. & Coulouvrat, F. 2002 Numerical simulation of sonic boom focusing. *AIAA J.* **40**, 1726–1734.

Baskar, S., Coulouvrat, F. & Marchiano, R. 2006 Irregular reflection of acoustical shock waves and von Neumann paradox. In *Proceedings of 17th International Symposium on Nonlinear Acoustics (in the press)*.

Ben-Dor, G. 1987 A reconsideration of the three-shock theory for a pseudo-steady mach reflection. *J. Fluid Mech.* **181**, 467–484.

Ben-Dor, G. 1992 *Shock Wave Reflection Phenomena*. Springer Verlag, New York.

Ben-Dor, G. & Takayama, K. 1985 Analytical prediction of the transition from Mach to regular reflection over cylindrical concave wedges. *J. Fluid Mech.* **158**, 365–380.

Ben-Dor, G. & Takayama, K. 1992 The phenomena of shock wave reflection - a review of unsolved problems and future research needs. *Shock Waves* **2**, 211–223.

Birkhoff, G. 1950 *Hydrodynamics, A Study in Logic, Fact and Similitude*. Princeton Univ. Press.

Brio, M. & Hunter, J. K. 1992 Mach reflection for the two-dimensional Burgers' equation. *Physica* D **60**, 194–207.

Colella, P. & Henderson, L. F. 1990 The von Neumann paradox for the diffraction of a weak shock waves. *J. Fluid Mech.* **213**, 71 – 94.

Coulouvrat, F. & Marchiano, R. 2003 Nonlinear Fresnel diffraction of weak shock waves. *J. Acoust. Soc. Am.* **114**, 1749 – 1757.

Courant, R. & Friedrichs, K. O. 1948 *Supersonic flows and shock waves*. Interscience.

Guderley, K. G. 1962 *The Theory of Transonic Flow*. Pergamon.

Hamilton, M. F. & Blackstock, D. T. 1998 *Nonlinear Acoustics*. Academic Press.

Henderson, L. F. 1987 Region and boundaries for diffracting shock wave systems. *Z. Angew. Math. Mech.* **67**, 73 – 86.

Henderson, L. F., Crutchfield, W. Y. & Virgona, R. J. 1997 The effects of thermal conductivity and viscosity of argon on shock waves diffraction over rigid ramps. *J. Fluid Mech.* **331**, 1–36.

Hunter, J. K. 1991 Nonlinear geometrical optics. In *Multidimensional hyperbolic problems and computations* (ed. A. J. Majda & J. Glimm), pp. 179 – 197. IMA Volumes in Mathematics and its Applications Vol. 29, Springer.

Hunter, J. K. & Brio, M. 2000 Weak shock reflection. *J. Fluid Mech.* **410**, 235 – 261.

Kobayashi, S., Adachi, T. & Suzuki, T. 1995 Examination of the von Neumann paradox for a weak shock wave. *Fluid Dyn. Res.* **17**, 13–25.

Kobayashi, S., Adachi, T. & Suzuki, T. 2004 Non-self-similar characteristics of weak Mach reflection: the von Neumann paradox. *Fluid Dyn. Res.* **35**, 275–286.

Lee, Y. S. & Hamilton, M. F. 1995 Time-domain modeling of pulsed finite-amplitude sound beams. *J. Acoust. Soc. Am.* **97**, 906–917.

Mach, E. 1878 Über den Verlauf von Funkenwellen in der Ebene und im Raume. *Sitzungsbr. Akad. Wiss. Wien* **78**, 819–838.

Marchiano, R., Coulouvrat, F. & Grenon, R. 2003 Numerical simulation of shock wave focusing at fold caustics, with application to sonic boom. *J. Acoust. Soc. Am.* **114**, 1758–1771.

Marchiano, R., Coulouvrat, F. & Thomas, J. L. 2005 Nonlinear focusing of acoustic shock waves at a caustic cusp. *J. Acoust. Soc. Am.* **117**, 566 – 577.

McDonald, B. E. & Kuperman, W. A. 1987 Time domain formulation for pulse propagation including nonlinear behavior at a caustic. *J. Acoust. Soc. Am.* **81**, 1406–1417.

von Neumann, J. 1943 Oblique reflection of shocks. In *John von Neumann collected work, vol 6, (1963)* (ed. A. H. Taub), pp. 238–299. Pergamon, New York.

Skews, B. W. 1972 The flow in the visinity of the three shock interaction. *CASI Trans.* **4**, 99–107.

Skews, B. W. & Ashworth, J. T. 2005 The physical nature of weak shock wave reflection. *J. Fluid Mech.* **542**, 105–114.

Sternberg, J 1959 Triple-shock-wave intersections. *Phys. Fluids* **2**, 179–206.

Tabak, E. G. & Rosales, R. R. 1994 Focusing of weak shock waves and the von Neumann paradox of oblique shock reflection. *Phys. Fluids* **6**, 1874 – 1892.

Takayama, K. & Ben-Dor, G. 1985 The inverse Mach reflection. *AIAA J.* **23**, 1853 – 1859.

Tesdall, A. M. & Hunter, J. K. 2002 Self-similar solutions for weak shock reflection. *SIAM. J. Appl. Maths.* **63**, 42–61.

Vasil'ev, E. & Kraiko, A. 1999 Numerical simulation of weak shock diffraction over a wedge under the von Neumann paradox conditions. *Comput. Maths. Math. Phys.* **39**, 1335–1345.

Zabolotskaya, E. A. & Khokhlov, R. V. 1969 Quasi-plane waves in the nonlinear acoustics of confined beams. *Sov. Phys. Acoust.* **15**, 35–40.

Zakharian, A. R., Brio, M., Hunter, J. K. & Webb, G. M. 2000 The von Neumann paradox in weak shock reflection. *J. Fluid Mech.* **422**, 193 – 205.